Journal of Power Sources 199 (2012) 360–366

Contents lists available at SciVerse ScienceDirect

Journal of Power Sources

journal homepage: www.elsevier.com/locate/jpowsour

Integration of batteries with ultracapacitors for a fuel cell hybrid transit bus

Piyush Bubna, Suresh G. Advani*, Ajay K. Prasad

Center for Fuel Cell Research, Department of Mechanical Engineering, University of Delaware, Newark, DE 19716, United States

ARTICLE INFO

Article history:
Received 30 August 2011
Accepted 28 September 2011
Available online 5 October 2011

Keywords:
Fuel cell hybrid electric vehicle
Battery
Ultracapacitor
Simulation
Lifetime

ABSTRACT

Battery electric vehicles and hybrid electric vehicles require electric energy storage systems that exhibit high energy and power density, as well as good cycle life. Batteries possess good energy density, whereas ultracapacitors possess high power density and cycle life. The complementary features of batteries and ultracapacitors can be advantageously combined to create an integrated system that exhibits high performance with low weight and adequate battery lifetime, at an affordable cost. This paper presents simulation studies on the benefits of adding ultracapacitors to a fuel cell battery hybrid transit bus operating on two standardized driving schedules (Manhattan Bus Cycle and UDDS). Simulations were conducted using our LFM powertrain simulator which was developed in MATLAB/SIMULINK. The energy storage systems considered here include battery only, as well as various combinations of batteries and ultracapacitors. Simulation results show that the addition of ultracapacitors greatly improves performance parameters such as battery *C*-rates, energy throughput, and energy storage heat generation at comparable cost and weight.

1. Introduction

Fuel cells have emerged as one of the most promising candidates for fuel-efficient and emission-free vehicle power generation. In particular, proton exchange membrane fuel cells have received much attention for automotive applications due to their low operating temperature and high power density. Although the primary barrier to the commercialization of fuel cells is their high cost, there are other operational hurdles that need to be overcome. In order to improve the transient performance of fuel cells, and to recover energy through regenerative braking, fuel cells are typically paired with reversible energy storage systems (ESS) to form hybrid power-trains. Such hybrid power-trains are particularly well suited for transit applications where the average power demand is low due to frequent starts and stops of the vehicle.

Batteries and ultracapacitors are the most commonly used ESS in hybrid electric vehicles. Batteries have much higher specific energy than ultracapacitors and can propel the vehicle for a longer time. On the other hand, ultracapacitors possess high specific power and can provide or accept large bursts of power during vehicle acceleration or a regenerative-braking event, respectively. Due to these complementary properties, batteries can be combined with ultracapacitors to create a lightweight, compact ESS that exhibits a good compromise between energy and power densities. Another significant difference between the two types of ESS is their lifetime. Batteries typically lose their effectiveness after a few thousand charge–discharge cycles. In contrast, ultracapacitors are able to maintain performance for about one million cycles. Table 1 compares the power density, energy density and life cycle characteristics of an advanced technology battery and an ultracapacitor [1,2]. Studies suggest that stress factors such as temperature, depth-of-discharge, current load (*C*-rate), throughput, and number of cycles affect battery lifetime [3–5]. Storage system lifetime is therefore another metric which can be enhanced by pairing a battery with an ultracapacitor which could alleviate battery stress by employing a smart energy management strategy.

Fuel cell/battery and fuel cell/ultracapacitor hybrids have been studied individually in light of their fuel economy, performance, and design and control strategy optimization [6–10]. Recent studies have also explored the combination of batteries and ultracapacitors for possible benefits in fuel economy, performance, and cost [11–17]. Furthermore, other studies have investigated battery stress reduction or battery life extension by combining batteries with ultracapacitors in PHEVs. For example, Schaltz et al. [18] studied the influence of lead-acid battery and ultracapacitor size on battery depth-of-discharge and hence battery life, as well as system volume, and mass. Burke and Zhao [19] demonstrated reduced battery current by combining ultracapacitors with lithium-ion and zinc-air batteries. Dougal et al. [20] have shown extended battery discharge life in the presence of ultracapacitors under pulse load conditions using simplified models.

This paper investigates the improvement in factors affecting battery lifetime by simulating the effect of adding ultracapacitors to a fuel cell battery hybrid transit bus operating on standard urban

* Corresponding author. Tel.: +1 302 831 8975; fax: +1 302 831 3619.
E-mail address: advani@udel.edu (S.G. Advani).

0378-7753/$ – see front matter © 2011 Elsevier B.V. All rights reserved.
doi:10.1016/j.jpowsour.2011.09.097

Table 1
Power density, energy density and cycle-life comparison of advanced technology batteries and ultracapacitors.

	Altairnano (LiTi cell)	Maxwell ultracapacitor
Peak[a]		
W kg^{-1}	760	5900
Wh kg^{-1}	72	5.96
Cycle life	>12,000 cycles at 100% DoD[b] (2*C* rate and 25 °C) >4000 cycles at 100% DoD (1*C* rate and 55 °C)	1 million cycles at 50% DoD

[a] Peak powers are calculated based on peak pulse currents of the ESS which may not be allowed by the traction inverter.
[b] Depth of discharge.

driving schedules. The specific performance parameters addressed are battery *C*-rates, battery throughput, and system as well as cell-level heat generation rates. Six different ESS combinations were simulated and compared in this study. In addition to the performance parameters mentioned above, the influence on energy storage cost and weight is also discussed. Simulations were performed using our in-house LFM software which is developed in MATLAB/SIMULINK. The vehicle platform simulated in this study was the University of Delaware fuel cell hybrid bus operating on two standard urban driving schedules (the Manhattan Bus Cycle and UDDS).

We begin by describing the vehicle, fuel cell, battery and ultracapacitors (Section 2), powertrain topology and energy management scheme (Section 3), followed by the simulation results (Section 4), and finally the conclusions (Section 5).

2. Vehicle configuration

The University of Delaware's Fuel Cell Hybrid Bus Program commenced in 2005 with the goal to research, build and demonstrate a fleet of fuel cell transit buses and hydrogen refueling stations in the state of DE [21]. Our Phase 2 fuel cell hybrid bus has been used as the vehicle platform for this study. This 22 ft bus is driven by a single three-phase AC induction motor that is rated for 130 kW peak and 100 kW continuous. The motor is coupled to the rear drive wheels through a single-speed chain drive and a differential. The vehicle is powered by dual fuel cell stacks described below, and battery energy storage. The curb weight of the bus including the fuel cell system but without the energy storage system is 6030 kg. Additional details about the bus and its on-board systems can be found in [21].

2.1. Fuel cell

The fuel cell system consists of dual Ballard Mark9 SSL stacks, each with 110 cells and a combined power rating of 38.8 kW. The hydrogen is stored in two composite high-pressure tanks located on the top of the bus. The tanks are rated for 350 bar and have a total storage capacity of approximately 12.8 kg of hydrogen.

2.2. Battery

The Phase 2 bus is currently equipped with NiCd batteries. However, for the present analysis we have considered the more advanced lithium-titanate batteries. Two different sizes of lithium-titanate batteries are considered: one string of 144 cells in series (denoted as 1xBatt), and two strings of 144 cells in series (denoted as 2xBatt). The cells are 50 Ah Altairnano lithium-titanate cells [1]. Each string of 144 cells weighs 360 kg, and has a maximum power of 120 kW and 16.5 kWh of available energy (Table 2). The cost of the cell was obtained from the vendor.

Table 2
Battery specifications.

Altairnano 144 cell pack (1xBatt)	
Number of cells	144
Max/min voltage	400/260 V
Max. current	300 A
Max. power	120 kW
Available energy	16.5 kWh
Capacity	50 Ah
Module weight	360 kg
Internal resistance	80 mOhm
Cost	$27,072

2.3. Ultracapacitors

Maxwell BCAP3000 ultracapacitor cells are considered in the present analysis [2]. Four different sizes of ultracapacitor packs have been considered for the simulation study and their details are given in Table 3. A 1xUcap module is made up of a stack of 40 cells in series and weighs 42.5 kg. The maximum power of the 1xUcap module is 30 kW while the available energy is 78 Wh. The maximum voltage, maximum power, energy and weight of the ultracapacitor pack scales linearly with its size. The energy storage and fuel cell models are described in [22].

2.4. DC/DC converter

A bi-directional DC/DC converter is considered in the simulations for a battery + ultracapacitor energy storage system. It has been assumed that the converter bucks/boosts voltage with a constant efficiency of 97%. Based on the listed DC/DC converter cost in [12], the ESS cost analysis in the latter part of this paper assumes an additional expense of $1500 for the DC/DC converter for each of the four cases studied. An average weight of 30 kg is assumed for the DC/DC converter based on a supplier's technical data for their bi-directional converter products [23].

3. Topology and energy management scheme

The present analysis considers two battery-only ESSs, and four combinations of battery and ultracapacitor which involve four different ultracapacitor sizes. The topology and energy management strategy are discussed below.

3.1. Battery-only ESS

The drivetrain topology for a fuel cell–battery series hybrid vehicle is shown in Fig. 1. Power from the battery and fuel cell feeds the traction motor and the accessory load. Note that power flow is bidirectional in the traction motor and battery. The battery can accept power from either the fuel cell, or the traction motor during regenerative braking. Two battery-only ESSs are considered in this study: 1xBatt and 2xBatt.

Table 3
Ultracapacitor specifications.

Maxwell BCAP3000 cells	1xUcap (40 cells)	2xUcap (80 cells)	3xUcap (120 cells)	4xUcap (160 cells)
Max/min voltage	100/50 V	200/100 V	300/150 V	400/200 V
Max. current	300 A	300 A	300 A	300 A
Max. power	30 kW	60 kW	90 kW	120 kW
Available energy	78 Wh	156 Wh	234 Wh	312 Wh
Capacitance	75 F	37.5 F	25 F	19 F
Internal resistance	11.6 mOhm	23.2 mOhm	34.8 mOhm	46.4 mOhm
Module weight	42.5 kg	85 kg	127.5 kg	170 kg
Cost	$3600	$7200	$10,800	$14,400

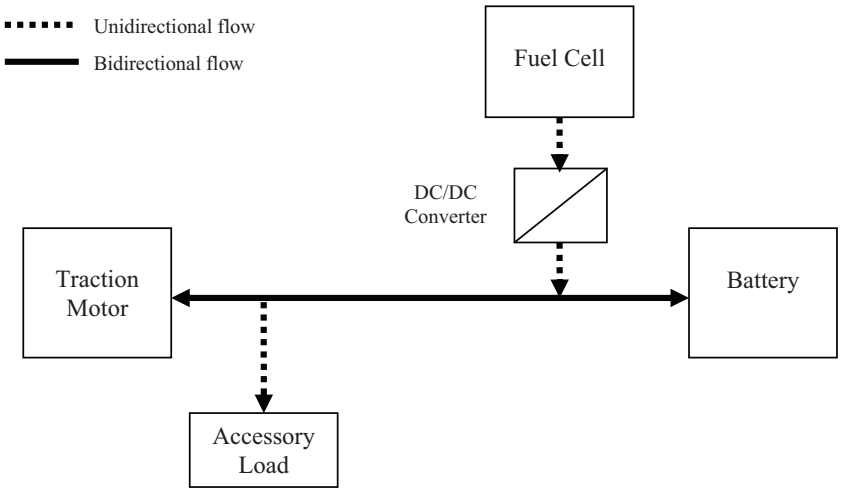

Fig. 1. Topology of a fuel cell/battery series hybrid.

3.1.1. Hybrid energy management

The fuel cell net power is given by [22]:

$$P_{FC,net} = P_{avg} + \alpha(SOC_d - SOC_c) \quad (1)$$

where P_{avg} is the combined power consumption of the traction motor and accessory load averaged over a moving time frame (1 h in this case), SOC_d is the state-of-charge to which the battery is desired to be depleted, and α is a constant in the correction term which alters the power request based on the deviation of the real time SOC (SOC_c) from the desired value.

The required battery power is given by

$$P_{battery} = P_{tract} + P_{acc} - P_{FC,net} \quad (2)$$

where P_{tract} and P_{acc} are the power consumption of the traction motor and accessory load, respectively. Note that P_{tract} is negative during regenerative braking.

3.2. Battery + ultracapacitor ESS

The topology of a fuel cell–battery–ultracapacitor series hybrid is shown in Fig. 2. The ultracapacitor is connected to the battery/traction motor bus through a bi-directional DC/DC converter to buck or boost its voltage. For this portion of the analysis, the system uses the same fuel cell and battery as in the case of the fuel cell–battery hybrid described in Section 3.1. Four battery and ultracapacitor combinations are considered in this study; the same 1xBatt battery is maintained in all four combinations, while the Ucap size ranges from 1xUcap to 4xUcap.

3.2.1. Hybrid energy management

The fuel cell net power remains unchanged in the present energy management scheme and is given by Eq. (1); it should be noted that the SOC here still refers to the *battery* state-of-charge. The transient power demand is shared between the battery and ultracapacitor. Since the ultracapacitor has limited available energy, it is best utilized during events of high power demand or supply corresponding to vehicle acceleration or regenerative-braking events, respectively. The role of the ultracapacitors during such events is to deliver or absorb energy at high rates and thereby relieving battery stress to a great extent. To perform this role effectively, the ultracapacitor should be charged up to full capacity during periods of low vehicle speed such that it is ready to provide power during acceleration. Conversely, during periods of high vehicle speed, the ultracapacitor should be at the lowest desired SOC in order to fully accept regenerative charge during a braking event. Therefore, in the current power management scheme, the ultracapacitor

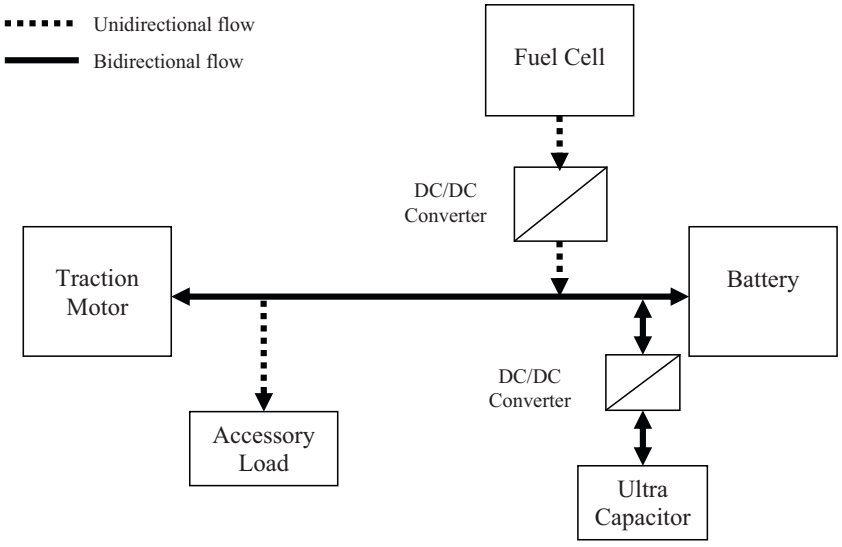

Fig. 2. Topology of fuel cell/battery/ultracapacitor series hybrid.

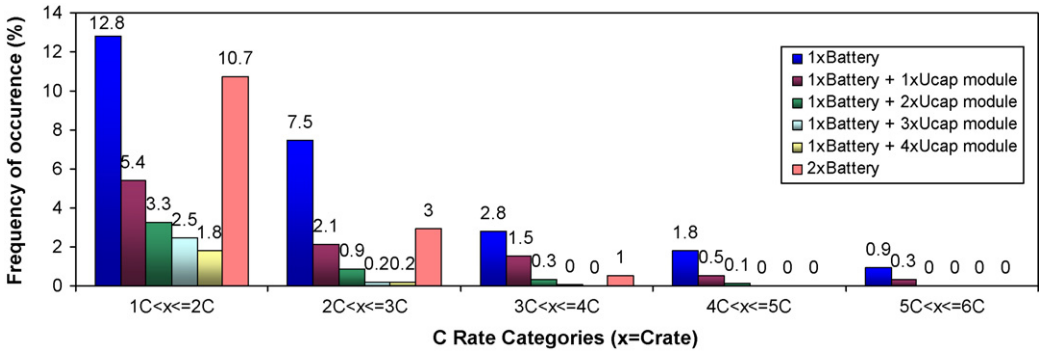

Fig. 3. Simulated battery *C*-rate frequency distribution for the six ESS combinations on the Manhattan Bus Cycle.

voltage is controlled based on the vehicle speed and a target voltage is calculated using the following equation [12].

$$\lambda \frac{1}{2} m v^2 + \frac{1}{2} C U_{\text{target}}^2 = \beta \tag{3}$$

with the following boundary values:

$$\begin{aligned} v &= 0 \ \text{ mph} \Rightarrow U_{\text{target}} = U_{\max} \\ v &= 57 \ \text{ mph} \Rightarrow U_{\text{target}} = U_{\min} \end{aligned} \tag{4}$$

Here $(1/2)mv^2$ is the kinetic energy of the vehicle, and $(1/2)CU_{\text{target}}^2$ is energy content of the ultracapacitor. C is the capacitance of the ultracapacitor pack as given by Table 3, and U is its voltage. λ and β are constants whose values are calculated from Eq. (3) by inserting the boundary values in Eq. (4). First, the value of β is obtained by noting that when the vehicle is stationary, the desired ultracapacitor voltage is set to the maximum allowable voltage, $U_{\max}$. Next, for the two drive cycles considered here, the peak velocity is 57 mph. Hence, the value of λ is obtained by setting the desired ultracapacitor voltage to the minimum allowable value, $U_{\min}$, at $v = 57$ mph.The ultracapacitor power request, P_{Ucap} is given by:

$$P_{\text{Ucap}} = P_{\text{ESS}} - K_{\text{p}}(U_{\text{target}} - U_{\text{current}}) \tag{5}$$

where P_{ESS} is the transient power demand from the battery and ultracapacitor combined and is given by:

$$P_{\text{ESS}} = P_{\text{tract}} + P_{\text{acc}} - P_{\text{FC,net}} \tag{6}$$

Here U_{current} is the current ultracapacitor voltage, U_{target} is the calculated desired ultracapacitor voltage given by Eq. (3), and K_{p} is a proportionality constant. The value of K_{p} is determined by requiring that the ultracapacitor generates an additional 4 kW power for a 10 V difference between the current and target ultracapacitor voltage; hence $K_{\text{p}} = 400$.

The term $K_{\text{p}}(U_{\text{target}} - U_{\text{current}})$ in Eq. (5) is a correction term which ensures that the ultracapacitor meets requested transient demands while adhering to the target voltage according to Eqs. (3) and (4). P_{Ucap} is the desired power from the ultracapacitor. If the ultracapacitor is undersized for the requested power demand (or supply), it will supply (or accept) its maximum rated power. Any excess power demand is met by the battery.

4. Simulation results

The ESS performance was simulated using our in-house powertrain simulator called LFM. This powertrain simulation tool has been comprehensively validated in previous studies [24]. The Manhattan Bus Cycle and UDDS were considered for this study. The Manhattan Bus Cycle is a milder drive cycle with mean and maximum velocities of 6.8 mph and 25.4 mph, respectively. In comparison, UDDS is a more aggressive cycle with mean and maximum velocities of 19.6 mph and 57 mph, respectively. Results for the two drive cycles are presented next.

4.1. Effect on C-rate and energy throughput

Fig. 3 shows the effect of ultracapacitors on battery current draw for various *C*-rate ranges for the Manhattan Bus Cycle. Fig. 3 indicates a reduction in the frequency of high *C*-rate current draws from the battery in presence of ultracapacitors. For example, the 1xBatt ESS (one of the two battery-only ESSs considered) experiences currents in the 2*C*–3*C* range during 7.5% of the Manhattan Bus Cycle. However, this frequency is reduced to only 2.1% when the battery is integrated with a 1xUcap module. With increasing number of ultracapacitor modules, their ability to share the transient current loads increases further. Fig. 3 shows that when the ESS includes a 4xUcap module, the battery never experiences currents exceeding 3*C* during the entire drive cycle. In sharp contrast, the 1xBatt ESS experiences periods at even the highest *C*-rate during some portion of the drive cycle. These results show that the ultracapacitor is extremely effective in shielding the battery from high *C*-rates, thereby reducing battery stress.

It is interesting to compare the 1xBatt + ultracapacitor ESSs with the battery-only 2xBatt ESS. Although Fig. 3 shows that the 2xBatt ESS does not experience *C*-rates in excess of 4*C*, it definitely undergoes substantial exposure to lower *C*-rates. In particular, the exposure of the 2xBatt to the 1*C*–2*C* range is not very different from the 1xBatt. The 2xBatt still sees currents in the 2*C*–3*C* range for about 3% of the drive cycle.

Fig. 4 shows that load sharing by the ultracapacitor also reduces the energy throughput of the battery pack. Energy throughput is defined as the sum of the magnitudes of energy flowing into and out of the battery during the drive cycle. Fig. 4 presents energy throughput data on a per-cell basis, and shows that the addition of even 1xUcap reduces the battery throughput by almost 50% for the Manhattan Bus Cycle. A lower value of throughput indicates that the battery is participating in energy transfer to a smaller extent, and is consequently incurring reduced stress.

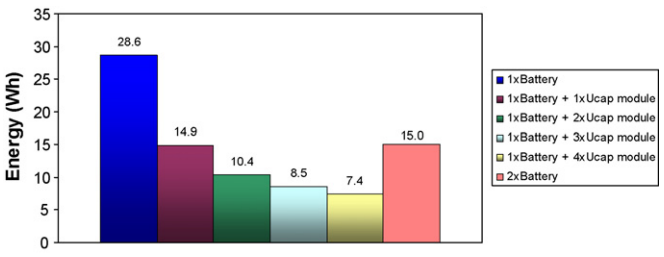

Fig. 4. Simulated energy throughput per battery cell for the six ESS combinations on the Manhattan Bus Cycle.

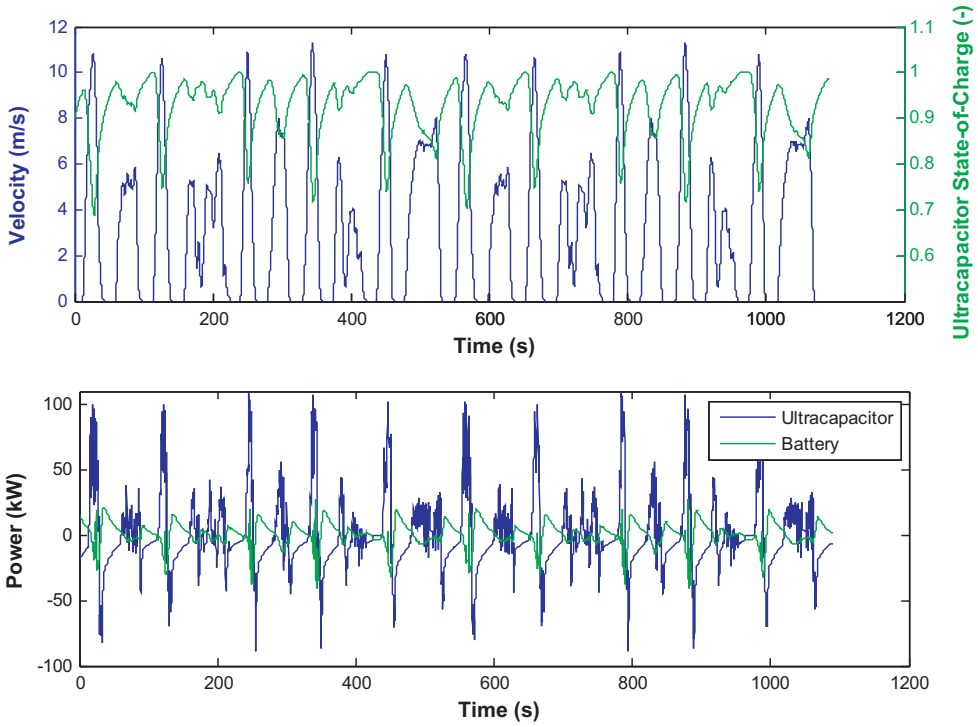

Fig. 5. Simulated velocity and power profiles on the Manhattan Bus Cycle for 1xBatt + 4xUcap ESS. Correlation between vehicle velocity and ultracapacitor SOC (top); battery and ultracapacitor power (bottom).

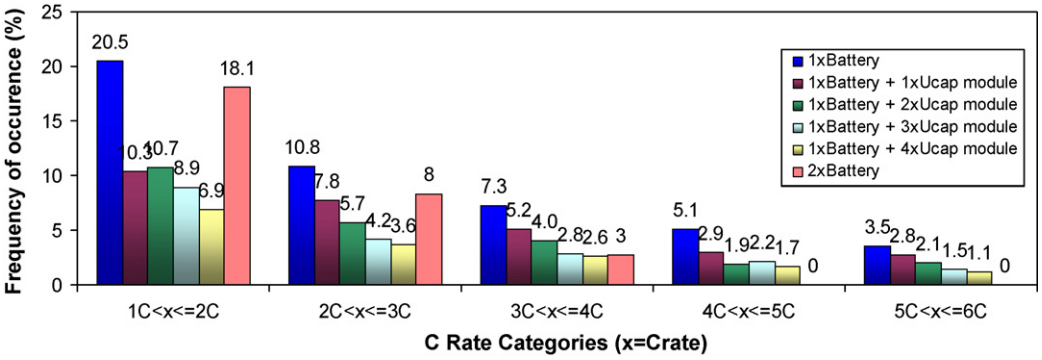

Fig. 6. Simulated battery *C*-rate frequency distribution for six different ESS combinations on the UDDS cycle.

It is important to note that the battery + ultracapacitor ESSs provide greater improvements in battery *C*-rates and energy throughput when compared to a battery-only ESS. In particular, integrating a 1xBatt + 4xUcap results in substantial improvement in *C*-rate and throughput performance, and is superior to that achieved by simply doubling the battery size (2xBatt).

The dramatic improvement in the *C*-rate frequency distribution with the 4xUcap module can be understood from Fig. 5. The power management strategy keeps the ultracapacitor at high SOC at low vehicle speeds and vice versa. As a result, the 4xUcap which has a maximum power of 120 kW, is able to meet the peak power demands which typically occur for short durations, while the battery provides or accepts low power levels. The effectiveness of ultracapacitors of smaller size is reduced because of power and energy limitations. For example, a 1xUcap module has 30 kW peak power and four times less available energy. Therefore, the battery is forced to participate more frequently and contribute to peak demands when it is integrated with a 1xUcap module.

The battery + ultracapacitor ESS is also quite effective on the UDDS cycle. However, because the UDDS is a much more aggressive cycle in comparison to the Manhattan Bus Cycle, the beneficial effects on battery *C*-rate (Fig. 6) and throughput reduction (Fig. 7) are somewhat reduced. Due to the higher power and energy demands of the UDDS, the 4xUcap module is unable to completely suppress battery currents in the 3*C*–6*C* range (Fig. 6). However, the 4xUcap module performs better than the 2xBatt ESS

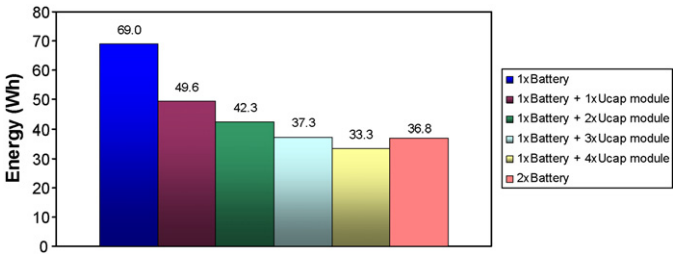

Fig. 7. Simulated energy throughput per battery cell for six different ESS combinations on the UDDS Cycle.

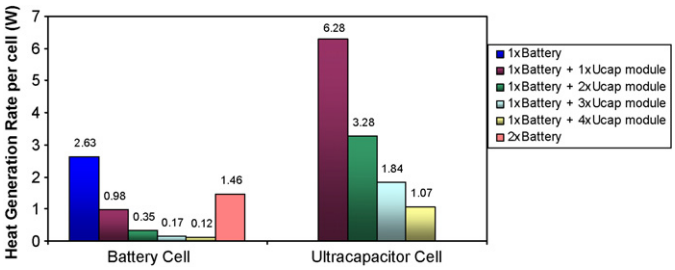

Fig. 8. Simulated heat generation rates for each battery and ultracapacitor cell averaged over the Manhattan Bus Cycle.

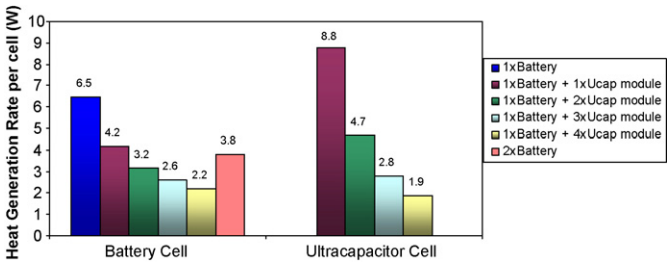

Fig. 9. Simulated heat generation rates for each battery and ultracapacitor cell averaged over the UDDS cycle.

in the 1C–2C current range and in terms of battery energy throughput.

4.2. Effect on heat generation

A direct consequence of the battery and ultracapacitor current profiles is their respective heat generation rates. Heat generation rates are presented on a per-cell basis for the battery and the ultracapacitor for the Manhattan Bus Cycle (Fig. 8) and UDDS (Fig. 9). Fig. 8 indicates that for the Manhattan Bus Cycle, the average heat generation rate in the Altairnano cell is reduced by up to 10 and 20 times by the addition of ultracapacitors when compared to 2xBatt and 1xBatt packs, respectively. This result convincingly demonstrates that the combination of an ultracapacitor pack with the battery permits huge reductions in battery cell heat generation while still maintaining or even reducing the weight of the ESS (Fig. 13).

The degree of reduction in battery heat generation is drive-cycle dependent. For UDDS, Fig. 9 shows that the battery cell heat generation in a 4xUcap-assisted ESS is only 1.7 and 3 times less than the 2xBatt and 1xBatt packs, respectively. Despite the smaller improvement in battery heat generation, it should be emphasized that reduction in heat generation rate is particularly beneficial for battery life because higher operating temperatures have a strong effect on battery degradation.

In comparison with the battery cells, the ultracapacitor cells are subjected to higher heat generation rates in both bus drive cycles (Figs. 8 and 9). In particular, cells within smaller ultracapacitor packs face higher currents and hence incur a higher average heat generation rate. Therefore, the thermal consequences on both the battery and ultracapacitor cells have to be considered while sizing the energy storage system. Figs. 10 and 11 depict the cumulative heat generation rate of the complete energy storage system. For larger ultracapacitor packs, the total heat generated by the ESS is minimized for both the drive cycles considered in this study. Lower thermal losses also imply higher system efficiency. Furthermore, since a lower heat generation is correlated with a larger ultracapacitor pack size, this also implies that more cell surface area is

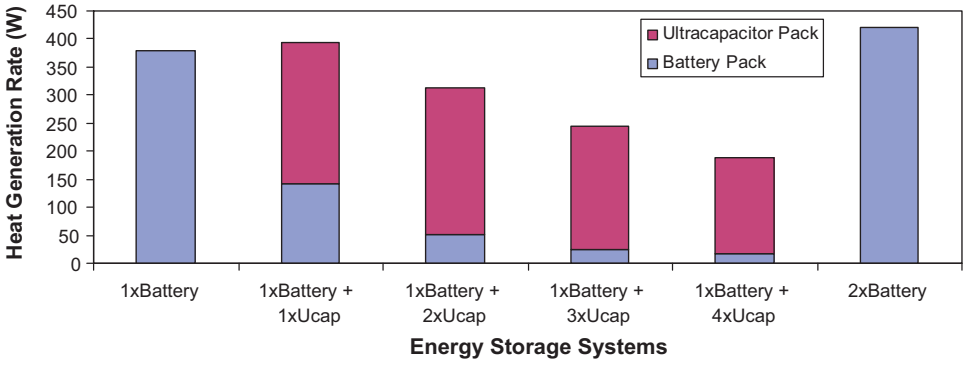

Fig. 10. Simulated cumulative heat generation rates for all six ESS combinations averaged over the Manhattan Bus Cycle.

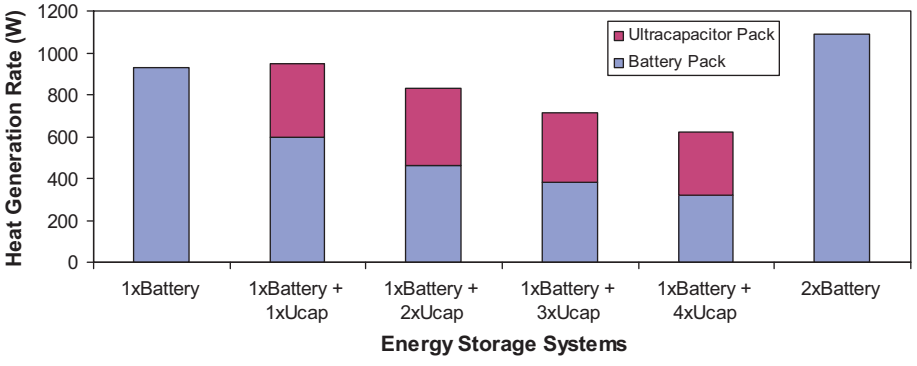

Fig. 11. Simulated cumulative heat generation rates for all six ESS combinations averaged over the UDDS cycle.

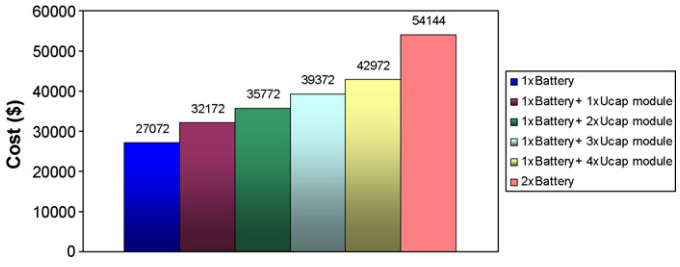

Fig. 12. Energy storage system cost.

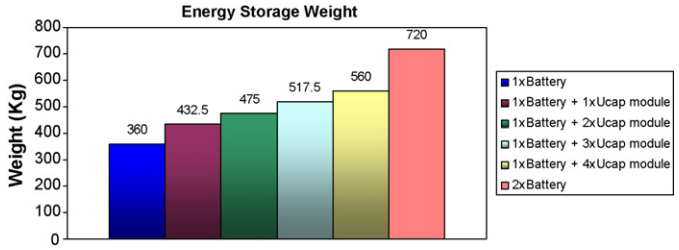

Fig. 13. Energy storage system weight.

available for heat dissipation, either through natural or forced convection. Consequently, the cell cooling system can be downsized and its parasitic power consumption can be reduced.

4.3. Effect on ESS cost and weight

In general, the 4xUcap pack demonstrates better, and in a few cases, similar results when compared to the 2xBatt ESS with respect to the following three parameters: *C*-rates, energy throughput, and heat generation. Moreover, these improvements are achieved at a lower energy storage cost and weight. Fig. 12 shows that while the 1xBatt ESS is the cheapest option, the 1xBatt + 4xUcap ESS is in fact cheaper than 2xBatt. Note that the cost of the DC/DC converter is included in the battery + Ucap cost in Fig. 12. Fig. 13 shows that weights of the various ESSs studied here follow the same trend as the cost. The weight of DC/DC converter is included in the battery + Ucap cost in Fig. 13. The study shows that benefits could be realized by investing resources and space on adding ultracapacitors to the battery pack rather than simply increasing the size of the battery.

One of the considerations in doubling the size of the battery pack is the associated reduction in the battery depth-of-discharge leading to an enhancement of battery lifetime. However, due to a charge-sustaining power-management strategy employed on our bus, and the energy configurations considered in the present study, the maximum depth-of-discharge on the 1xBatt pack is very low – 1% on the Manhattan Bus Cycle and 7% on UDDS. The vehicle weight with the fuel cell but without the ESS is 6030 kg. For the different ESS sizes considered in this study, the maximum difference in weight is 360 kg which is about 5% of the total vehicle weight. Therefore, vehicle energy consumption is not significantly impacted by differences in ESS weight. The influence of ESS size on vehicle weight, and hence energy consumption, would be more significant if the heavier lead-acid or nickel-based batteries were considered for this study.

5. Summary and conclusions

This paper presents a simulation study that explores the concept of battery-load reduction by integrating ultracapacitors within the electric energy storage system. Six different energy storage sizes/combinations are considered and the corresponding power management strategies are presented. Simulations results indicate a significant improvement in battery *C*-rates, energy throughput, and cell heat generation rate due to the addition of ultracapacitor packs to the battery. In most cases, the performance of a battery + ultracapacitor ESS is superior to that of a dual battery pack and at lower cost and weight. Therefore, it can be concluded that the integration of ultracapacitors into the ESS permits the downsizing of the battery pack resulting in cost and weight savings without compromising battery lifetime. Simulation studies also indicate that the magnitude of improvement in performance with an ultracapacitor is drive-cycle dependent. Therefore, in addition to battery-lifetime goals and cost, the selection of an appropriate ultracapacitor pack size also depends on the expected battery usage (duty cycle). A comprehensive battery-life model can bring more perspective to such studies and help to extend the use of simulations to actual decision making.

Acknowledgement

This research was sponsored by the Federal Transit Administration.

References

[1] Altairnano 24 V 50 Ah datasheet <http://www.targetdoc.com/viewer.asp?b=546&k=lchr4714LC&bhcp=1>.
[2] Maxwell K2 series datasheet <http://www.maxwell.com/docs/DATASHEET_K2_SERIES_1015370.PDF>.
[3] X.G. Yang, B. Taenaka, T. Miller, K. Snyder, International Journal of Energy Research 34 (2010) 171–181.
[4] <http://www.nrel.gov/vehiclesandfuels/energystorage/pdfs/48933_smith.pdf>.
[5] <http://www.nrel.gov/vehiclesandfuels/energystorage/pdfs/46031.pdf>.
[6] P. Rodatz, G. Paganelli, A. Sciarretta, L. Guzzella, Control Engineering Practice 13 (2005) 41–53.
[7] M.J. Kim, H. Peng, Journal of Power Sources 165 (2007) 819–832.
[8] V. Paladini, T. Danteo, A. Risi, D. Laforgia, Energy Conversion and Management 48 (2007) 3001–3008.
[9] V. Paladini, T. Donateo, A. Risi, D. Laforgia, Journal of Fuel Cell Science and Technology 5 (2008) 1–8, 021004 (May).
[10] R.K. Ahluwalia, X. Wang, A. Rousseau, Journal of Power Sources 152 (2005) 233–244.
[11] D. Gao, Z. Gin, Q. Lu, Journal of Power Sources 185 (2008) 311–317.
[12] J. Bauman, M. Kazerani, IEEE Transactions on Vehicular Technology 57 (2008) 760–769.
[13] W. Gao, IEEE Transaction on Vehicular Technology 54 (2005) 846–855.
[14] R. Schupbach, J. Balda, M. Zolot, B. Kramer, Proceedings of IEEE Power Electronics Specialist Conference 1 (2003) 88–93.
[15] G. Pede, A. Iacobazzi, S. Passerini, A. Bobbio, G. Botto, Journal of Power Sources 125 (2004) 280–291.
[16] A. Baisden, A. Emadi, IEEE Transaction on Vehicular Technology 53 (2004) 199–205.
[17] M. Zandi, A. Payman, J.P. Martin, S. Pierfederici, B. Davat, F.M. Tabar, IEEE Transaction on Vehicular Technology 60 (2011) 433–443.
[18] E. Schaltz, A. Khaligh, P.O. Rasmussen, IEEE Transactions on Vehicular Technology 58 (2009) 3882–3891.
[19] A. Burke, H. Zhao. <http://www.its.ucdavis.edu/people/faculty/burke/index.php>, 2010.
[20] R.A. Dougal, S. Liu, R.E. White, IEEE Transactions on components and packaging technologies 25 (2002) 120–131.
[21] P. Bubna, D. Brunner, J.J. Gangloff Jr., S.G. Advani, A.K. Prasad, Journal of Power Sources 195 (2010) 3939–3949.
[22] P. Bubna, D. Brunner, S.G. Advani, A.K. Prasad, Journal of Power Sources 195 (2010) 6699–6708.
[23] <http://ushybrid.com/BDC2.pdf, http://ushybrid.com/BDC4.pdf>.
[24] D. Brown, M. Alexander, D. Brunner, S.G. Advani, A.K. Prasad, Journal of Power Sources 183 (2008) 275–281.